



## Constraining the Origin and Age of the Thermal and Cold Water in the Lake Natron Basin, Northern Tanzania

Edista A. Abdallah<sup>1\*</sup>, Charles H. Kasanzu<sup>1</sup>, Crispin P. Kinabo<sup>1</sup>, Akira Imai<sup>2</sup> and Mike J. Butler<sup>3</sup>

<sup>1</sup>Department of Geosciences, University of Dar es Salaam, P.O. Box 35052, Dar es Salaam, Tanzania.

<sup>2</sup>Department of Earth Resources Engineering, Kyushu University, Japan.

<sup>3</sup>iThemba Laboratory, Private Bag 11, Wits, 2050, Johannesburg, South Africa.

Email addresses: [abdister@udsm.ac.tz](mailto:abdister@udsm.ac.tz); [kcharls16@yahoo.com](mailto:kcharls16@yahoo.com); [kinabo\\_2003@yahoo.co.uk](mailto:kinabo_2003@yahoo.co.uk); [imai@mine.kyushu-u.ac.jp](mailto:imai@mine.kyushu-u.ac.jp); [mj.butler@ilabs.nrf.ac.za](mailto:mj.butler@ilabs.nrf.ac.za).

\*Corresponding author

Received 18 Aug 2022, Revised 31 Oct 2022, Accepted 13 Nov 2022, Published Dec 2022

DOI: <https://dx.doi.org/10.4314/tjs.v48i4.8>

### Abstract

Springs on the eastern and western shores of Lake Natron Basin (LNB), located within the eastern branch of the East Africa Rift System (EARS) in Northern Tanzania had a discharge temperature that ranged between 34.0 °C and 51.2 °C, while the pH varied from 8.0 to 10.7. The electrical conductivity (EC) ranged between 5,007 µS/cm and 49,200 µS/cm. Cold waters had a temperature of 31.9 °C to 32.5 °C, while the pH ranged between 8.0 and 8.3, and the EC ranged between 1,401 µS/cm and 3,806 µS/cm. The stable isotope composition varied between -2.4 ‰ and -5.3 ‰ for δ<sup>18</sup>O, and -15.5 ‰ to -29.3 ‰ for δ<sup>2</sup>H. The isotopic composition of thermal and cold water of LNB indicates a significant contribution of meteoric water in the recharge of the hydrothermal system. However, thermal water is affected by evaporation, water-rock interaction, carbon dioxide (CO<sub>2</sub>) exchange and condensation processes. Tritium analysis indicated that the spring water in the LNB hydrothermal system has a residence time of more than 50 years.

**Keywords:** thermal water; Lake Natron Basin; stable isotopes; springs.

### Introduction

Stable isotope compositions of thermal waters are valuable indicators of a wide range of geological conditions related to hydrothermal reservoirs (Craig 1963, Karolytè et al. 2017). There are many applications of stable isotopes in characterising thermal waters including determination of the origin of water, residence time, subsurface mixing, migration, recharge elevation, reservoir temperature and water-rock interaction (Truesdell et al. 1977, D'Amore and Panichi 1985, Delalande et al. 2011, Wang et al. 2018). Due to the

difference in mass, stable isotopes behave differently in physical and geochemical processes. Variations in the isotopic composition may provide information about the natural processes controlling the fractionation of stable isotopes of oxygen (<sup>18</sup>O) and hydrogen (<sup>2</sup>H) in thermal water.

In order to constrain such dynamics on thermal waters, we investigated the Lake Natron Basin (LNB) which is a sedimentary basin located within the eastern branch of the East Africa Rift System (EARS) in Tanzania (Dawson 2008). Due to the active rifting and volcanic activities, the basin has several

thermal and cold springs running perpendicular to the border fault, small springs and clusters of large seeps and springs that drain towards Lake Natron (Hochstein et al. 2000 Muirhead et al. 2016). The hot springs of LNB have previously been documented by Hochstein (1999), who mapped the hydrothermal systems of the whole EARS and classified them according to their characteristics. Lake Natron's hydrothermal system was classified as an advective brine system of low temperature occurring in the arid climate region (Hochstein 1999, Hochstein et al. 2000). Hochstein et al. (2000) postulated that heat from the upper crustal rocks is swept by meteoric water infiltrating the higher rift shoulders, attaining in part their mineral content by leaching the surrounding sediments containing evaporites.

Lee et al. (2016) interpreted the soil CO<sub>2</sub> flux of Magadi-Natron basins (Kenyan-Tanzanian border) as being related to magma derived from the mantle and upper crust. On the other hand, Muirhead et al. (2016) used the fault population data and lava chronology to investigate the evolution of fault-related strains during the early stages of rifting in the Magadi-Natron basins. Furthermore, the geochemistry of thermal springs was used to examine the role of magmatic volatile released in the rift basin evolution. It was found that the thermal fluids are responsible for weakening the faults and assisting in strain localisation, thus the location of thermal springs in the Magadi-Natron basins coincides with areas of high strain (Muirhead et al. 2016).

This study presents a detailed investigation of stable isotopes of thermal and cold spring waters in LNB. The objective is to understand the isotopic compositions of thermal and cold waters of the LNB. The study also reports sub-surface processes affecting isotopic signatures of thermal and cold waters in the region and characterises the thermal springs in terms of origin and age in order to understand the dynamics of hydrothermal systems in the area.

## **Geological setting**

The EARS runs from the Afar junction in Ethiopia southward through Kenya, Tanzania and Malawi to Mozambique and is regarded as one of the largest known continental rifts in the region (Dawson 2008, Macgregor 2015). This is a typical example of an active continental rift caused by extensional faulting, magmatism and thinning of the lithosphere (Ring 2014, Muirhead et al. 2016).

The Tanzanian rift segment forms the southernmost branch of the eastern branch. This zone is called the Northern Tanzania Divergence (NTD) zone (Ebinger et al. 1989, Foster et al. 1997) (Figure 1). The NTD hosts three rifts of different orientations. In the western part, it consists of two rift branches, the Natron-Manyara-Balangida and Eyasi-Wembere rifts, and in the eastern part, the Pangani Rift. Within each rift, several distinctive basins are formed filled up with lake sediments intercalated with lava flows and ash-fall deposits (Dawson 2008, Ring 2014). This study focused on the Lake Natron Basin (LNB) located at the northern end of the Tanzanian-Kenyan border; just 30 km from Lake Magadi in Kenya and around 200 km from Arusha town in Tanzania.

## **Local geology**

The geology of the study area in LNB is summarised in Figure 2. It is mainly controlled by major tectonic processes including faulting and volcanism of the EARS (Dawson 2008, Neukirchen et al. 2010). The basin sedimentation was terminated by an approximately 20 km long Natron boundary faulting forming an eastern part-facing escarpment on the west of the basin (Figure 2). On the east occurs the extinct shield volcano, followed by undulating hills towards north to the Kenyan border (Dawson, 2008, Muirhead et al. 2016). To the south occurs the active volcano; Oldoinyo Lengai (Dawson 2008). Neogene volcanic rocks belong to the olivine-basalt-trachyte-phonolite association. They are assigned to Pleistocene to Recent. Basalts are common rock type including porphyritic basalts, olivine basalts and

basanites. The basalts underlie the Middle Pleistocene Peninj Group sediments and are well exposed in the rift scarps probably derived from the Oldonyo Sambu volcano (Guest and Pickering 1966a, Dawson 2008). Trachytes are also common believed to be contemporaneous with the final activity of Gelai volcano in the east of the basin. The

lenses of massive tuff and agglomerate are locally interbedded with the basaltic lavas and tuff cones are exposed in the rift wall NNE of Pinyinyi village. Phonolite composed of nepheline and sanidine is reported to occur in both volcanoes (Guest and Pickering 1966).

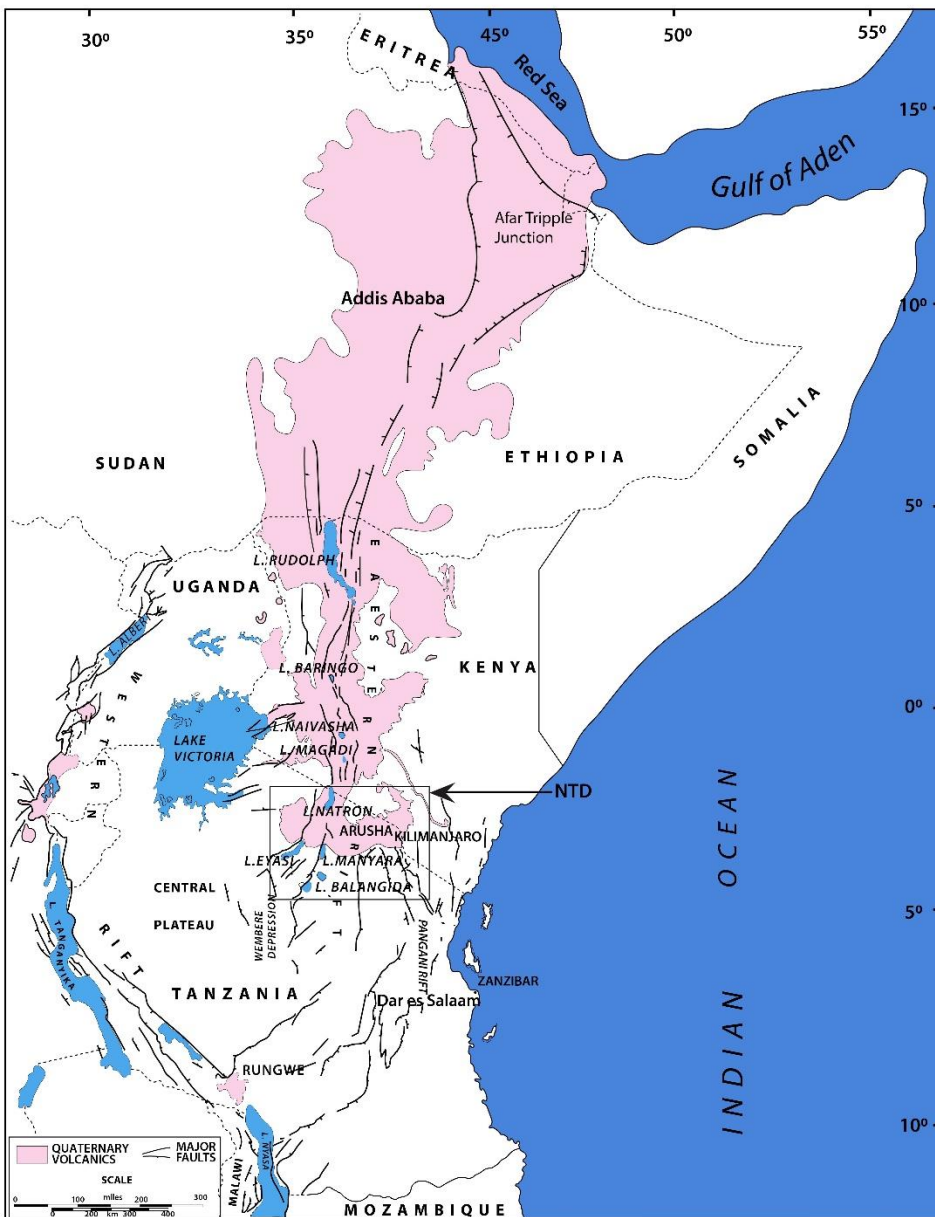


**Figure 1:** Map of East Africa, showing the East Africa Rift System and the location of the Northern Tanzania Divergence (NTD) zone.

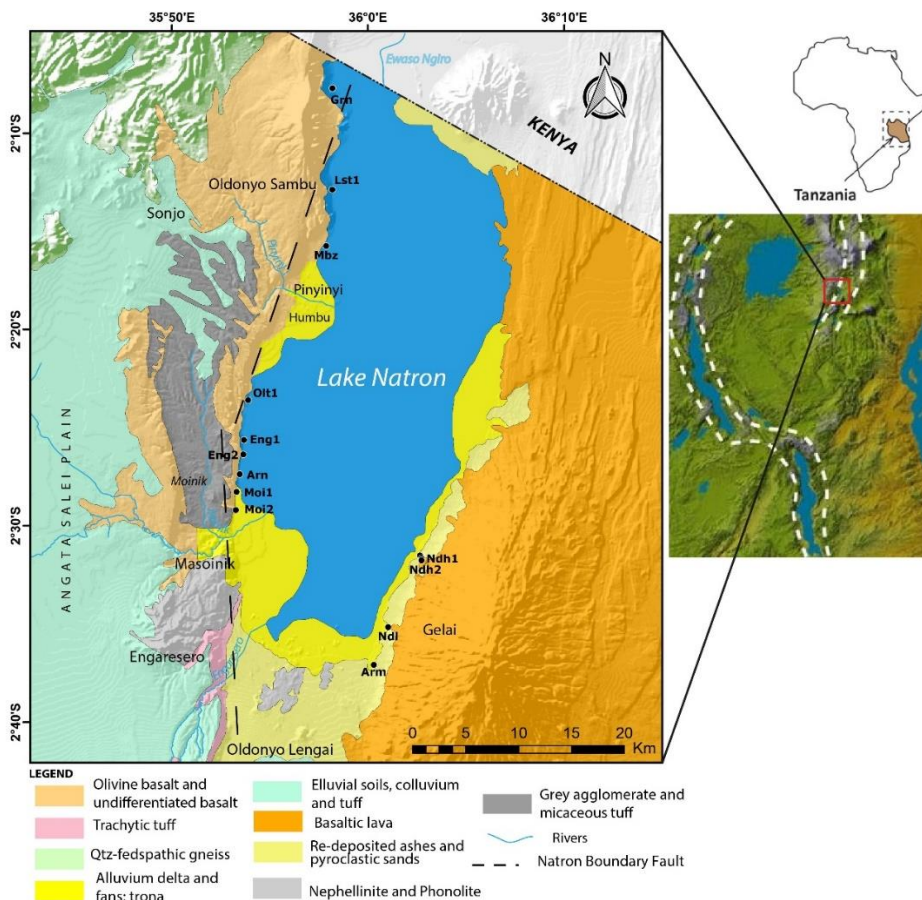


**Figure 2:** Map showing a summarised geology of Lake Natron Basin in northern Tanzania. Black dots are the sampling locations (modified after Guest et al. 1961, Guest and Pickering 1966b).

## Materials and Methods

### Sampling and analysis

Ten thermal ( $N = 10$ ) springs and two ( $N = 2$ ) cold springs water samples were collected at the study area between January and February 2021 to document the variability in stable isotope ratios of  $\delta^{18}\text{O}$  and  $\delta^2\text{H}$ . Temperature ( $T$ ), electrical conductivity ( $EC$ ) and  $\text{pH}$  were measured *in situ* using YSI multi-parameter instrument before collection of water samples. The samples were collected in flint glass bottles ( $N = 12$ ) according to Arnórsson et al. (2006) procedures. The sampling took place at an altitude ranging from 604 to 630 m above sea level in the LNB. Sample locations are indicated in

Figure 2. The sampling locations are based on the accessibility of the hot springs. In addition, three water samples were collected in 1 litre International Atomic Energy Agency (IAEA) plastic bottles for tritium ( $^3\text{H}$ ) analysis.

Stable isotopes of oxygen and deuterium; and tritium were analysed at the Environmental Isotope Laboratory (EIL) of iThemba Labs, Johannesburg, South Africa by an instrument consisting of a Los Gatos Research (LGR) Liquid Water Isotope Analyser. Each batch of samples were analysed with the laboratory standards that were calibrated against international reference materials with an analytical

precision estimated at 0.5 ‰ for  $^{18}\text{O}$  and 1.5 ‰ for  $^2\text{H}$ . The analytical results are presented in the common delta-notation (equation 1) expressed as per mil deviation to mean Vienna-standard mean oceanic water (V-SMOW) for  $\delta^{18}\text{O}$  and  $\delta^2\text{H}$ . The following equation was used:

$$\delta_{\text{sample}} = \left( \frac{R_{\text{sample}}}{R_{\text{std}}} - 1 \right) \times 1000 \quad (1)$$

where  $R_{\text{sample}}$  is the ratio of sample and  $R_{\text{std}}$  is the ratio of standard both measured in parts per thousand (‰) and reported as delta ( $\delta$ ) notation. The results are presented in Table 1.

The tritium samples were analysed as follows: 500 ml of tritium water samples were initially distilled and subsequently enriched by electrolysis to produce a corresponding enrichment factor of about 20. Analysis was done by a Liquid Scintillation Counter where samples are prepared by directly distilling the enriched water sample from the highly concentrated electrolyte. 10 ml of the distilled water sample was mixed with 11 ml Ultima Gold and placed in a vial in a Packard Tri-Carb 3170TR/SL Liquid Scintillation Analyser and counted 2 to 3 cycles of 4 hours. Detection limits were 0.2 TU for the enriched sample.

## Results

Physical parameters and the stable isotope ( $\delta^{18}\text{O}$  and  $\delta^2\text{H}$ ) ratios of western and eastern LNB thermal and cold water are presented in Table 1. The highest surface temperature of 51.2 °C was measured at Olajata (Olt1) thermal spring, while the lowest temperature is 34 °C measured at Arng'arwa (Arn) thermal spring. pH varies between 8.0 and 10.7 at Ndahane (Ndh2) and Lesiteti (Lst1) thermal springs. High electrical conductivity (EC) of 49,200  $\mu\text{S}/\text{cm}$  was observed at Gerleni (Grn) thermal spring, while the lowest EC was 5,007  $\mu\text{S}/\text{cm}$  measured at Engongowasi (Eng2) thermal spring. For the cold springs, the highest temperature recorded was 32.5 °C at Moiniki (Moi2) and

the lowest was 31.9 °C at Moi1. The pH ranged between 8.0 and 8.3; and the EC ranged between 1,401  $\mu\text{S}/\text{cm}$  and 3806  $\mu\text{S}/\text{cm}$  at Moi1 and Moi2, respectively.

Stable isotopes composition of LNB waters are plotted in the  $\delta^{18}\text{O} - \delta^2\text{H}$  diagram (Figure 3) relative to local meteoric water line (LMWL) with  $\delta^2\text{H} = 7.17\delta^{18}\text{O} + 7.36$  and Global Meteoric Water Line (GMWL) with  $\delta^2\text{H} = 8x + 10$  as defined by Craig (1961). The LMWL for Tanzania was estimated by using precipitation data from IAEA website recorded in 1960 to 1979 at Dar es Salaam, the coastline station located in latitude 06° 52' S and longitude 39°12' E, at an elevation of 55 m above sea level. Lugodisha et al. (2020) and Mckenzie et al. (2010) used almost similar LMWL  $\delta^2\text{H} = 7.03\delta^{18}\text{O} + 7.05$  and  $\delta^2\text{H} = 7.05\delta^{18}\text{O} + 7.0$  in the studies of Arusha and Mount Kilimanjaro aquifers, respectively.

On the  $\delta^{18}\text{O} - \delta^2\text{H}$  diagram (Figure 3), almost all the samples lie close to GMWL and LMWL an indication that they are likely of meteoric origin. Few samples, e.g. Eng1, Eng2, Arn1 and Olt1, lie close to GMWL and LMWL, while Moi1 and Moi2 lie close to LMWL but on top of GMWL. The stable isotope shifts away from both LMWL and GMWL were observed in the thermal waters samples of Grn, Lst1 and Mbazi (Mbz) indicating an influence of evaporation, while little interaction of thermal water with the reservoir rocks was indicated by samples Lst1 and Mbz increasing a little amount of  $\delta^{18}\text{O}$  but not  $\delta^2\text{H}$ . It was noted that stable isotope ratios of the thermal waters of West Lake Natron Basin (WLNB) vary systematically towards south end of the lake. The  $\delta^2\text{H}$  ratios in WLNB range between -15.5‰ in Grn and -29.3‰ in Moi2, whereas  $\delta^{18}\text{O}$  ratios ranged between -2.4 ‰ in Grn and -5.3 ‰ in Moi2. The Moi1, Moi2, Eng1 and Eng2 are the most depleted samples plotted on the bottommost part of the diagram (Figure 3) probably indicating the effect of condensation.

**Table 1:** Isotopic composition of LNB thermal and cold waters

Local name	ID	Coordinates		Altitude (m)	Temperature (°C)	pH	EC (μS/cm)	δ <sup>2</sup> H (‰)	δ <sup>18</sup> O (‰)	<sup>3</sup> H (TU)
		Latitude	Longitude							
Gerleni	Grn	2°07'37"S	35°58'11"E	612	35.9	10.3	49,200	-15.5	-2.4	-
Lesiteti	Lst1	2°12'48"S	35°58'11"E	610	39.4	10.7	12,100	-21.8	-3.5	0.0
Mbazi	Mbz	2°15'40"S	35°57'52"E	611	36.4	9.1	14,530	-21.4	-3.4	0.0
Olajata	Olt1	2°23'33"S	35°53'53"E	602	51.2	9.5	25,300	-26.8	-4.3	0.4
Engongowasi	Eng1	2°25'35"S	35°53'40"E	611	41.9	9.8	14,100	-28.2	-4.9	-
Engongowasi	Eng2	2°26'19"S	35°53'38"E	604	37.2	9.2	5,007	-27.5	-4.9	-
Arng'arwa	Arn	2°27'19"S	35°53'27"E	608	34	9.3	10,480	-25.4	-4.3	-
Moiniki	Moi1	2°28'14"S	35°53'17"E	607	31.9	8.3	1,401	-28.5	-5.2	-
Moiniki	Moi2	2°29'09"S	35°53'15"E	616	32.5	8.9	3806	-29.3	-5.3	-
Ndalesindai	Ndl	2°35'08"S	36°01'02"E	630	35.7	8.8	7,693	-23.9	-4.9	-
Ndahane	Ndh1	2°31'37"S	36°02'44"E	613	38	8.4	9,580	-23.1	-4.8	-
Ndahane	Ndh2	2°31'37"S	36°02'45"E	618	37.9	8.0	9,622	-23.5	-4.9	-

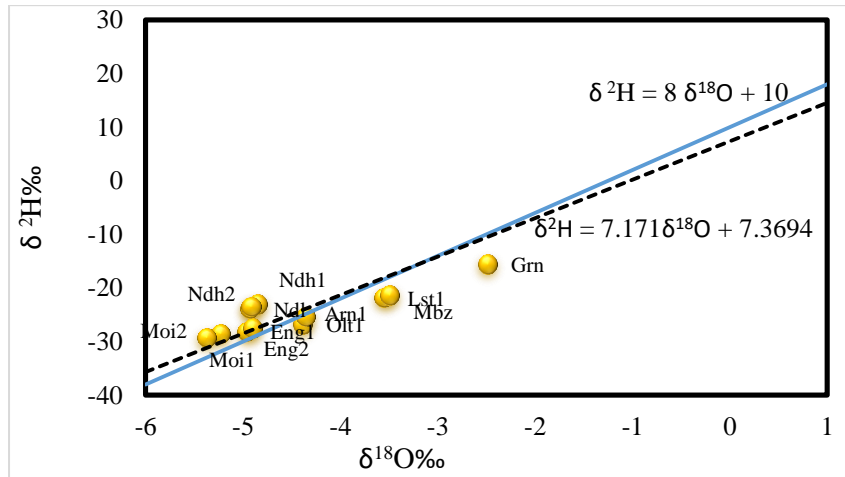


**Figure 3:** A plot of δ<sup>18</sup>O and <sup>2</sup>H values of thermal waters of the LNB in reference to Global Meteoric Water Line (GML) and Local Meteoric Water Line (LMWL) (IAEA/WMO 2007).

Thermal waters of the Eastern Lake Natron Basin (ELNB) indicated little or no variation in ratios of  $\delta^{18}\text{O}$  and  $\delta^2\text{H}$ . The isotope ratios ranged between -4.8‰ and -4.9‰ and -23.1‰ and -23.9‰, respectively indicated by samples Ndh1, Ndh2 and Ndl from Ndahane and Ndalesindai thermal

springs. The samples plotted slightly above the MWLs a sign of a negative oxygen shift. Figure 4 is an example of carbonate rock in the Ndahane thermal spring resulted from precipitation of low temperature hydrothermal minerals in the study area.



**Figure 4:** An outcrop of carbonate rock precipitated in Ndahane thermal spring. The outcrop is a typical example of secondary hydrothermal mineral precipitation at low-temperature.

## Discussions

### Sources of thermal and cold waters in LNB

The origin of thermal and cold water can be traced via stable ratios  $^{18}\text{O}/^{16}\text{O}$  and  $^2\text{H}/^1\text{H}$  (Craig 1963, Petrini et al. 2013, Wang et al. 2018). The stable isotope values of the LNB plotted relative to the GMWL and LMWL exhibited correlation as an indication of the meteoric origin of the thermal waters despite the extremely high salinity. The cold water samples (Moi1 and Moi2) and thermal water samples (Eng1, Eng2, Arn1 and Olt) plot along or close to the meteoric water lines, suggesting that the water originated exclusively from local precipitation without an additional significant input from other sources. The LNB samples are enriched with stable isotopes of  $^{18}\text{O}$  and  $^2\text{H}$  that are consistent with isotope ratios of -4.4 ‰ to -3.7 ‰ and -28.9 ‰ to -21.5 ‰ for  $\delta^{18}\text{O}$  and  $\delta^2\text{H}$  as reported by Lee et al. (2016).

Although the isotopic composition indicated meteoric origin, the scattering around the meteoric water line suggests that the isotopic signature is modified by

evaporation, condensation, and subsurface processes. Some of the samples (e.g. Olt, Lst, Mbz and Grn) plot below the MWLs. This suggests evaporation prior to recharge that led to discrimination of  $^{18}\text{O}$  and  $^2\text{H}$  against  $^{16}\text{O}$  and  $^1\text{H}$ , thus heavier isotopes are partitioning into the remaining waters (Clark and Fritz 1997). Evaporation is extremely high in the LNB and it is suggested to be a major process for water loss in the basin (Dawson 2008).

Possible mixing of meteoric water with the magmatic influx may occur during ascent of the magmatic fluids through fault systems. Although, according to Lee et al. (2016) magmatic water is isotopically heavier than the values reported in this study making it impossible to be a source of thermal water in the study area. It is likely that thermal water in the LNB is a mixture of meteoric water infiltrating the rift wall, groundwater and Lake Natron water.

### Processes controlling isotopic composition of thermal and cold waters in LNB

Thermal and cold waters plotted on the GMWL and LMWL show the distribution of the isotope ratios and help to identify processes affecting the waters (Nicholson, 1993). Figure 5 presents processes affecting the thermal and cold waters of LNB. Evaporation of water at the surface or at shallow depths results in enrichment in  $^{18}\text{O}$  and  $^2\text{H}$  relative to the meteoric water. Evaporation is identified as a major process affecting the isotopic composition of thermal and cold water in the LNB. It is indicated in Figure 5 that some thermal springs in the basin have been highly affected by

evaporation where both  $^{18}\text{O}$  and  $^2\text{H}$  contents of thermal water are enriched. The ratios of isotopes of  $\delta^{18}\text{O}$ - $\delta^2\text{H}$  plotted in reference to meteoric lines showed significant evaporation forming an evaporation line that deviates from the meteoric water line with a slope of 4. Schwartz and Zhang (2003) suggested the slope of the evaporation line normally ranges from one to five. High evaporation was observed in Grn, Lst1 and Mbz thermal springs as compared to other springs in the basin. This is possibly caused by the location of the thermal springs in the rift floor and the fact that LNB is a closed basin where the lake water is circulating within the same basin environment triggering high evaporation.

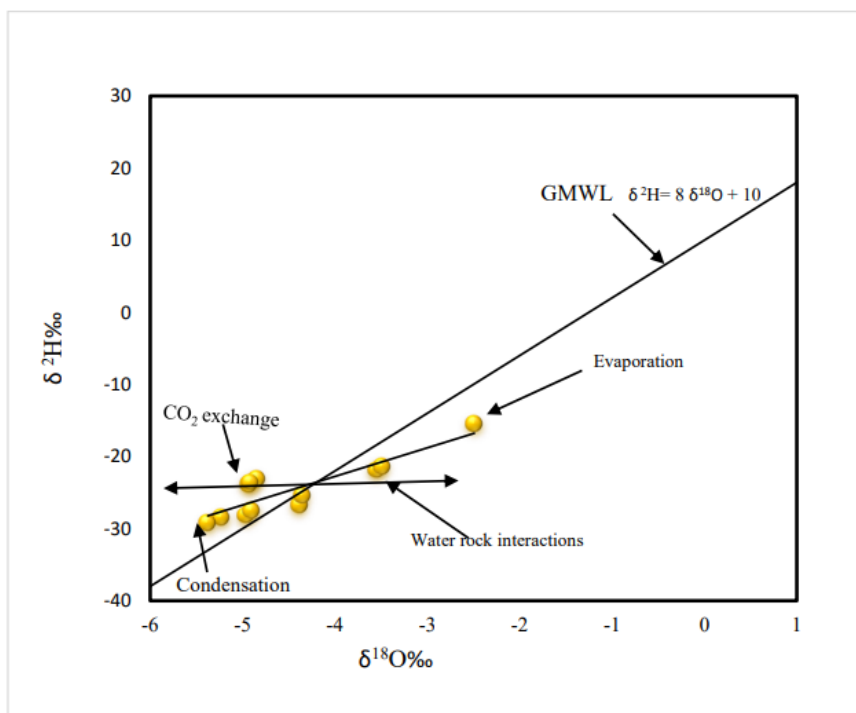


**Figure 5:** Processes controlling stable isotope composition of thermal waters in the LNB.

Apart from evaporation, some thermal springs (e.g. Mbz and Lst) show a slight positive  $^{18}\text{O}$  shift that can be attributable to a high-temperature isotopic exchange between the thermal water and silicate or carbonate host rocks which increases  $^{18}\text{O}$  in water (Craig 1963, Nicholson 1993). This process however is unnoticeable due to the deep  $\text{CO}_2$  reservoir related to the carbonatitic volcano

of Oldoinyo Lengai. The  $\text{CO}_2$  offsets the water rock exchange process by consuming the  $^{18}\text{O}$  in water leaving out the water that is poor in  $^{18}\text{O}$  (Craig 1963, Karolytė et al. 2017). High EC values (Table 1) in the basin are typical indicators of interaction between water and the host rocks (e.g., Benavente et al. 2016). The extent of oxygen shift is proportional to the difference in original  $\delta^{18}\text{O}$

between water and rocks, mineralogy, reservoir temperature and residence time; and inversely proportional to the water-rock ratio (Schwartz and Zhang 2003, Joseph et al. 2011). This process favours old systems with long contact time and a high water-rock ratio where the host rock reacts extensively with fluids to approach equilibrium with respect to oxygen exchange (Nicholson 1993, Wang et al. 2018).

Thermal waters from ELNB; Ndh1, Ndh2 and Ndl plots slightly above the MWLs showing a negative  $^{18}\text{O}$ -shift possibly related to the exchange between  $^{18}\text{O}$  of thermal water and  $\text{CO}_2$  rising through the faults (e.g. D'Amore and Panichi 1985, Lee et al. 2016). This is a common process in areas characterised by natural  $\text{CO}_2$  degassing like in active and dormant volcanoes, major fault zones, geothermal systems and thermal decomposition of organic matters (Karolytè et al. 2017, Mechal et al. 2017). In the LNB area, these characteristics are apparent and have been reported to exhibit massive emission of mantle-derived  $\text{CO}_2$  of about  $4 \text{ Mt yr}^{-1}$  as estimated from soil  $\text{CO}_2$  flux measurements (Lee et al. 2016). The faulting systems related to the EARS in LNB provide a local pathway through which  $\text{CO}_2$ -rich fluids are transported from the magma chamber (Lee et al. 2016, Muirhead et al. 2016, Lee et al. 2017).

The cold water (Moi1 and Moi2) and thermal water (Eng1 and Eng2) are the most depleted samples plotted on the bottommost part of the diagram (Figure 5). These waters are having their sources from precipitation and from dilute shallow groundwater. They are more dilute in terms of physical parameters, and their isotopic composition indicates more of meteoric, affected by the condensation process. Condensation is the most important process for the isotopic composition of precipitation (Dansgaard 1964). According to Dansgaard (1964), the first small amount of water condensed from vapour in equilibrium with SMOW will have the same composition as SMOW. In further condensation, the vapour preferentially loses heavy components, for the remaining vapour

and for newly formed condensate both getting more and more negative.

### **Age of thermal and cold water in the Lake Natron Basin robust**

Analysis of tritium content of thermal waters in LNB indicated that thermal water had a low T content of about 0–0.4 Tritium Unit (TU). Considering this, it can be suggested that the thermal waters in the LNB are T-free. The thermal water of LNB has been interacting with the host rocks for a long time such that tritium was not detected in two out of the three samples ( $T = 0 \text{ TU}$ ), however, one sample indicated 0.4 TU which is also subtle. This suggests that the age of the thermal fluids in LNB is older than 50 years. Mckenzie et al. (2010) reported similar results when attempting to determine the age of groundwater in the NTD region in Kilimanjaro. According to Mckenzie et al. (2010), the groundwater at the base of Mount Kilimanjaro such as that found at Miwaleni springs ( $T < 0.3 \text{ TU}$ ) originates from a regional source that has had a long time to interact with host rocks. Based on the findings by Mckenzie et al. (2010), fluid mineral content and stable isotope compositions presented in Table 1, it appears that LNB water was impacted by the high degree of water-rock reaction, resulting in a high solute content.

### **Conclusions**

The isotope ratios of thermal and cold waters in the LNB indicated that thermal and cold waters are of meteoric origin. Nevertheless, the isotopic ratios have scattered around the meteoric water line indicating that the water has been modified by evaporation and subsurface processes including  $\text{CO}_2$  exchange and water-rock interactions. It is expected that a high-temperature exchange reaction with silicate or carbonate minerals, should selectively result in an increase in  $^{18}\text{O}$  content, which would lead to a positive  $^{18}\text{O}$  shift. On the contrary, the high  $\text{CO}_2$  in the system offsets this process through an equilibrium isotope exchange reaction, which consumes the  $^{18}\text{O}$  while leaving out water deprived of  $^{18}\text{O}$ .

Moreover, the long residence time of water in the hydrothermal system indicated by tritium and the high EC values suggest possible interactions between water and the host rocks. The study agrees with earlier studies that the recharge originates from local groundwater, rift flanks and local precipitation. It is estimated that the hydrothermal systems in the LNB are older than 50 years.

### Acknowledgements

This research was funded by the Tanzanian Ministry of Education Science and Technology under MoEST Scholarship. The authors thank the anonymous reviewers for their helpful comments. Authors also extend acknowledgements to the Chief Editor of Tanzania Journal of Science, Prof. J.A.M. Mahugija, for handling the review processes and providing valuable inputs.

### References

- Arnórsson S, Bjarnason JÖ, Giroud N, Gunnarsson I and Stefánsson A 2006 Sampling and analysis of geothermal fluids. *Geofluids*. 6: 203-216.
- Benavente O, Tassi F, Reich M, Aguilera F, Capecchiacci F, Gutiérrez F, Vaselli O and Rizzo A 2016 Chemical and isotopic features of cold and thermal fluids discharged in the Southern Volcanic Zone between 32.5°S and 36°S: Insights into the physical and chemical processes controlling fluid geochemistry in geothermal systems of Central Chile. *Chem. Geol.* 420: 97-113.
- Clark I and Fritz P 1997 Environmental isotopes in hydrogeology. CRC Press, New York.
- Craig H 1961 Isotopic variations in meteoric water. *Science* 133(8): 1702-1703.
- Craig H 1963 The isotopic geochemistry of water and carbon in geothermal areas. In: *Nuclear Geology in Geothermal Areas*. pp 17-53, Spoleto Laboratorio di Geologia Nucleare, Pisa, Italy.
- D'Amore F and Panichi C 1985 Geochemistry in geothermal exploration. *Int. J. Energy Res.* 9: 277-298.
- Dawson JB 2008 The Gregory Rift Valley and Neogene–Recent volcanoes of Northern Tanzania. *Geol. Soc. Lond. Mem.* 33.
- Delalande M, Bergonzini L, Gherardi F, Guidi M, Andre L, Abdallah I and Williamson D 2011 Fluid geochemistry of natural manifestations from the Southern Poroto-Rungwe hydrothermal system (Tanzania): preliminary conceptual model. *J. Volcanol. Geotherm. Res.* 199: 127-141.
- Dansgaard W 1964 Stable isotopes in precipitation. *Tellus* XVI. 4: 466-468.
- Ebinger CJ, Deino AL, Drake RE and Tesha AL 1989 Chronology of volcanism and rift basin propagation–Rungwe Volcanic Province, East Africa. *J. Geophys. Res.* 94: 15785-15803.
- Foster A, Ebinger C, Mbede E and Rex D 1997 Tectonic development of the northern Tanzanian sector of the East African Rift System. *J. Geol. Soc. Lond.* 154: 689–700.
- Guest NJ and Pickering R 1966a Brief explanation of the geology of Kibangaini. QDS028, *Geological Survey of Tanzania*.
- Guest NJ and Pickering R 1966b Brief explanation of the geology of Gelai and Ketumbeine. QDS040, *Geological Survey of Tanzania*.
- Guest NJ, James T, Pickering R and Dawson J 1961 Brief explanation of the geology of Angata Salei. QDS039, *Geological Survey of Tanzania*.
- Hochstein MP 1999 Geothermal systems along the East-African Rift. *Bull. d'Hydrogeol.* 17: 301-310.
- Hochstein MP, Temu EP and Moshy CMA 2000 Geothermal resources of Tanzania. In: *Proceedings World Geothermal Congress, Kyushu-Tohoku*, 1233-1238.
- IAEA/WMO 2007 Global network of isotopes in precipitation. In: *The GNIP Database*. <http://isohis.iaea.org>. Cited in March 2012.
- Joseph EP, Fournier N, Lindsay JM and Fischer TP 2011 Gas and water geochemistry of geothermal systems in Dominican Island arc. *J. Volcanol. Geotherm. Res.* 206(1-2): 1-14.

- Karolytè R, Serno S, Johnson G and Gilfillan SMV 2017 The influence of oxygen isotopes exchange between CO<sub>2</sub> and H<sub>2</sub>O in natural CO<sub>2</sub>-rich spring waters: Implications for geothermometry. *J. Appl. Geochem.* 84: 173-186.
- Lee H, Muirhead JD, Fischer TP, Ebinger CJ, Kattenhorn SA, Sharp ZD and Kianji G 2016 Massive and prolonged deep carbon emission associated with continental rifting. *Nat. Geosci.* 9: 145-149.
- Lee H, Fischer TP, Muirhead JD, Ebinger CJ, Kattenhorn SA, Sharp ZD, Kianji G, Takahata N and Sano Y 2017 Incipient rifting accompanied by the release of subcontinental lithospheric mantle volatiles in the Magadi and Natron basin, East Africa. *J. Volcanol. Geotherm. Res.* 346: 118-133.
- Lugodisha I, Komakech HC, Nakaya S, Takada R, Yoshitani J and Yasumoto J 2020 Evaluation of recharge areas of Arusha aquifer, Northern Tanzania: application of water isotope tracers. *Hydrol. Res.* 51(6): 1490-1505.
- Macgregor D 2015 History of the development of the East African Rift System: A series of interpreted maps through time. *J. Afr. Earth Sci.* 101: 232-252.
- Mckenzie JM, Mark BG, Thompson LG, Schotterer U and Lin PN 2010 A hydrogeochemical survey of Kilimanjaro (Tanzania): implications for water sources and ages. *Hydrogeol. J.* 18: 985-995.
- Mechal A, Birk S, Dietzel M, Leis A, Winkler G, Mogessie A and Kebede S 2017 Groundwater flow dynamics in the complex aquifer system of Gidabo river basin (Ethiopian Rift): a multi-proxy approach *Hydrogeol. J.* 25: 519-538.
- Muirhead JD, Kattenhorn SA, Lee H, Mana S, Turrin BD, Fischer TP, Kianji G, Dindi E and Stamps DS 2016 Evolution of upper crustal faulting assisted by magmatic volatile release during early-stage continental rift development in the East African Rift. *Geosphere* 12(6): 1670-1700.
- Nicholson K 1993 Geothermal fluids: geochemistry and exploration techniques. Springer-Verlag, Berlin Heidelberg.
- Neukirchen F, Finkenbein T and Keller J 2010 The Lava sequence of the East African Rift escarpment in the Oldoinyo Lengai–Lake Natron sector, Tanzania. *J. Afr. Earth Sci.* 58 (5): 734-751.
- Petrini R, Italiano F, Ponton M, Slejko FF, Uviani U and Zini L 2013 Geochemistry and isotope geochemistry of the Monfalcone thermal water (northern Italy): inference on the deep geothermal reservoir. *Hydrogeol. J.* 21: 1275-1287.
- Ring U 2014 The East African Rift System. *Austrian J. Earth Sci.* 107(1): 132-146.
- Schwartz FW and Zhang H 2003 Fundamentals of groundwater. John Wiley & Sons, Inc. New York.
- Truesdell AH, Nathenson M and Rye RO 1977 The effects of subsurface boiling and dilution on the isotopic compositions of Yellowstone thermal waters. *J. Geophys. Res.* 82: 3964-3704.
- Wang X, Lu G and Hu B X 2018 Hydrogeochemical Characteristics and Geothermometry Applications of Thermal Waters in Coastal Xinzhou and Shenzao Geothermal Fields, Guangdong, China. *Geofluids* 2018 (8715080): 1-24.